Article

Numerical Evaluation of the Influence of Using Carbon-Fiber-Reinforced Polymer Rebars as Shear Connectors for Cross-Laminated Timber–Concrete Panels

Larissa Fé Alves [1,*], Poliana de Melo Pessôa [1], Pedro Ignácio Lima Gadêlha Jardim [1], Emerson Faustino [2], Herisson Ferreira dos Santos [2], Francisco Antonio Rocco Lahr [3], Diego Henrique de Almeida [1] and André Luis Christoforo [1]

1   Department of Civil Engineering, Federal University of São Carlos (UFSCar), Rod. Washington Luís, Km 235-SP-310, São Carlos 13565-905, Brazil; polianamelo@estudante.ufscar.br (P.d.M.P.); pedrojardim@estudante.ufscar.br (P.I.L.G.J.); diegoalmeida@unir.br (D.H.d.A.); alchristoforo@ufscar.br (A.L.C.)
2   Federal Institute of Education, Science and Technology of Rondônia (IFRO), Rodovia, RO-257, s/n-Zona Rural, Ariquemes 76870-000, Brazil; emerson.faustino@ifro.edu.br (E.F.); herisson.santos@ifro.edu.br (H.F.d.S.)
3   Department of Structural Engineering, University of São Paulo (USP), Av. Trabalhador São Carlense, 400, São Carlos 13566-590, Brazil; frocco@sc.usp.br
*   Correspondence: larissafe@estudante.ufscar.br

Abstract: Carbon fiber-reinforced polymer (CFRP) sheets have been used to reinforce cross-laminated timber (CLT)–concrete systems in recent years. The existing studies have indicated that the use of CFRP rebars as shear connectors in CLT–concrete panels can improve the structural performance of these elements. However, the application and understanding of CFRP rebars as shear connectors still need to be improved, since comprehensive studies on the subject are not available. Therefore, this research aimed to evaluate the structural performance of CLT–concrete panels with CFRP rebars as shear connectors through finite element (FE) numerical simulation. A parametric study was conducted, varying the connector material, the number of CLT layers, the connector insertion angle, and the connector embedment length. According to the results, panels with CFRP connectors showed a higher maximum load, bending strength, and maximum bending moment than panels with steel connectors. The regression models revealed that the parameters analyzed explained between 80.2% and 99.9% of the variability in the mechanical properties under investigation. The high explanatory power (R^2) of some regression models in this study underscores the robustness of the models. The number of CLT layers and the connector material were the most significant parameters for the panels' maximum load, displacement at the maximum load, ductility, bending strength, and maximum bending moment. The number of CLT layers and the connector insertion angle were the most significant parameters for the panels' effective bending stiffness. This research highlights the importance of studies on CLT–concrete composites and the need to develop equations to estimate their behavior accurately. Moreover, numerical simulations have proven very valuable, providing results comparable to laboratory results.

Keywords: CLT–concrete; shear connectors; numerical simulation; carbon-fiber-reinforced polymer (CFRP); bending performance; mechanical properties

1. Introduction

In recent years, the construction industry has sought to replace mineral-based products with sustainable wooden construction alternatives, aiming for better use of renewable resources, greater industrialization, and reduced production time [1]. In this scenario, cross-laminated timber (CLT) emerges as a structural material with enormous potential for application in medium- and high-rise buildings such as the four-story John W. Olver

Design Building at the University of Massachusetts Amherst [2] and the twenty-story Sara Kulturhus building in Skellefteå, reaching 75 m in height [3].

The CLT panel is formed by layers of sawn wood stacked and glued crosswise [4]. The interleaved assembly of the timber fiber direction in CLT elements can reduce anisotropic behavior and increase the timber's structural integrity [5]. These panels have advantages such as a high strength/weight ratio, which result in reduced foundation loads [6]. The growing interest in CLT is also associated with its qualities, such as structural resistance, environmental sustainability, and efficiency in construction processes [7]. However, concerning structural stability and performance in the face of vibrations, this material still requires further investigation to be used satisfactorily [8].

Incorporating a layer of concrete over CLT can address the limitations found in CLT floors and conventional reinforced concrete, resulting in a superior performance compared to individual materials [9]. This results in the formation of a CLT–concrete composite, also called timber concrete composite (TCC), which combines the main properties of each material. The upper part, made of concrete, offers resistance to compression forces, while the lower part, made of timber, is exceptionally resistant to bending and tensile stresses [10].

In TCC structures, the transmission of efforts between the two materials occurs due to the shear connectors, which allow relative sliding between the parts of this construction system. Therefore, a CLT–concrete composite system is considered partially composite, meaning that the timber and concrete elements will not be subject exclusively to compressive or tensile stresses [11]. As a result, the structural efficiency of a TCC system depends significantly on the stiffness of the connection between elements. The stiffer the connection, the greater the level of composite action, and consequently, the lower the vertical deformation of the structure under transverse loading [12].

Mechanical connectors (or shear connectors) are responsible for transferring shear stresses between timber and concrete. Various connection elements, such as plates, notches, dowel-type connectors, adhesives, and others, can be used to bond timber and concrete elements [12]. Inclined screws are a solution that is attracting interest due to the speed of execution. Furthermore, reducing the angle between the screw and the shear plane can provide optimal shear strength, as it maximizes the screw's withdrawal capacity [13]. The most significant mechanical properties of the connection are load capacity, stiffness, and ductility. Therefore, shear connections must be evaluated based on these properties [12].

Several studies have been carried out to investigate the influence of the connector insertion angle on the structural performance of CLT–concrete panels [10–12,14,15]. The embedment length of mechanical connectors has also recently been a studied parameter [8,10,12,16]. According to Bao et al. [8], the embedding depth of screws in CLT can significantly affect the shear performance of connectors. Furthermore, the thickness of CLT panels is also a parameter that affects the bending stiffness and strength of CLT and CLT–concrete structures [8,17]. Other parameters that influence the load transfer efficiency and structural stiffness include the connector configuration [13], connector spacing [11,15], and the types of connectors used [8,10,15,18]. Moreover, the durability and resistance of connectors to environmental factors also influence the longevity and maintenance of TCC structures.

Mai, Park, and Lee [10] conducted push-out tests to study the performance of connections in CLT–concrete systems. They considered parameters such as the types of connectors, concrete thickness, connector angle, and connector embedment length. Mirdad, Chui, and Tomlinson [11] performed a four-point bending test to assess the structural behavior of TCC structures. Their study involved various construction parameters including concrete thickness, insulation thickness, span, connector angle, and spacing. Furthermore, Mirdad and Chui [12] conducted shear tests to characterize connection stiffness and strength of TCC with different screw embedment lengths and angles.

In another study, Marchi, Scotta, and Pozza [13] investigated the mechanical behavior of inclined self-tapping screws used as TCC connectors in both single and crossed configurations through push-out tests. Mai et al. [15] conducted dynamic and four-point bending tests on CLT–concrete floors with various connector angles, types, and spacing

to evaluate their vibration characteristics and strength capacity. Furthermore, Shahnewaz, Jackson, and Tannert [16] investigated CLT–concrete floors with steel kerf plates as shear connectors through small-scale shear tests, varying the embedment depths of the connectors. Subsequently, two full-scale CLT–concrete floors were tested through four-point bending tests.

In a study by Morrell et al. [18], four types of shear connectors in CLT–concrete floors were investigated through push-off and three-point bending tests. The connectors included self-tapping screws, a modified lag screw with an integral plate washer, a steel angle anchored only at the end of the span, and an inverted-T steel section with stem perforations. Shahnewaz, Jackson, and Tannert [19] conducted experimental tests on CLT–concrete floors through small-scale shear tests. CLT–concrete floors connected with self-tapping screws, steel kerf plates, and Holz-Beton-Verbund (HBV) shear connectors were tested under four-point bending.

The most widely accepted analytical approach for TCC structures is the so-called gamma method. This method assumes that the shear connectors are uniformly distributed across the span. The accuracy of the results depends on parameters such as the γ factor, which measures the connection efficiency between the layers [20]. Obtaining these parameters requires experimental testing and calibrations, which may not be readily available or easy to perform in all contexts.

The gamma method is limited in its ability to evaluate the influence of specific parameters of shear connectors, such as connector material, diameter, non-uniform distribution, embedding length, and inclination angle. These limitations stem from the inherent simplifications in the method, which assumes a uniform distribution and average properties of the connectors along the CLT–concrete interface.

More detailed approaches are necessary to consider the influence of connector properties and other parameters on the behavior of CLT–concrete structures. Numerical models, such as the finite element method (FEM), can complement the gamma method and capture variations in behavior due to specific parameters. This approach allows consideration of the mechanical properties of materials and interactions between structural components. Additionally, it is possible to perform parametric analyses to evaluate the impact of different materials and connector configurations on system behavior.

The recent studies of Bao et al. [8], Mai, Park, and Lee [10], and Jiang and Crocetti [20] have explored this approach. Numerical analysis offers several advantages, including flexibility and versatility, allowing for rapid modification of parameters and loading conditions. It reduces costs and time while providing a detailed understanding of structural behavior. These characteristics make finite element simulations a valuable tool for investigating TCC systems.

In Japan, Canada, the United States, and European countries, research into alternative materials to steel has been actively conducted, with fiber-reinforced polymer (FRP) composites being used promisingly. FRP materials are widely used in the construction industry due to their notable mechanical and physical advantages, such as high chemical and corrosion resistance, lightweight, and non-conductivity. Among FRPs, carbon fiber-reinforced polymer composite (CFRP) has higher tensile strength and elastic modulus than steel rebars [21].

CFRP composites have high tensile and shear strengths and stiffness [22], so they are commonly used to reinforce timber and CLT–concrete structures [23,24]. Hadigheh et al. [6] and Hadigheh and Dias-da-Costa [22] highlighted the potential of CFRP as a viable option to achieve more efficient connections in CLT–concrete structures.

Even with all the potential applications of CLT–concrete structural elements, it is still necessary to deepen the understanding of the mechanics of these systems, especially concerning shear connections and the use of CFRP as a mechanical connector. The study by Hadigheh et al. [6] demonstrated improved structural performance in CLT–concrete beams when CFRP rebars were used as shear connectors. However, no other studies on this topic are currently available, and the individual physical and geometrical variables within this

structural system have not been separately analyzed. Understanding the impact of these variables on structural performance is crucial for making this a viable solution.

To this end, it is essential to develop parametric studies and parameter sensitivity analyses to understand how the parameters affect the structure's behavior and identify which parameters have the most significant impact on CLT–concrete performance. This approach allows designers to focus their optimization efforts on the most relevant variables. Furthermore, developing equations that predict the mechanical properties of CLT–concrete structures based on specific parameters can enable fast and accurate analysis during the design phase.

Systematic Literature Review and Research Justification

A systematic review was conducted using two scientific databases, Scopus and the Web of Science. The keywords listed in Table 1 were combined using the Boolean operators "AND" and "OR". English publications were considered without restrictions regarding the publication period to encompass all existing publications on this topic. Four publication prospecting conditions were used, including a general condition (General) established to identify studies on TCC structures whose timber element is CLT. Additionally, three specific search conditions were used to identify studies on CLT-concrete and CFRP (Specific I), parametric studies of CLT-concrete systems (Specific II), and sensitivity analysis of CLT-concrete system parameters (Specific III).

Table 1. Conditions and respective keywords.

Condition	String
General	("timber concrete composite") AND ("cross laminated timber" OR "cross-laminated timber")
Specific I	("timber concrete composite") AND ("cross laminated timber" OR "cross-laminated timber") AND ("carbon fiber reinforced polymer" OR CFRP)
Specific II	("timber concrete composite") AND ("cross laminated timber" OR "cross-laminated timber") AND parametric
Specific III	("timber concrete composite") AND ("cross laminated timber" OR "cross-laminated timber") AND sensitivity

Each of the strings was investigated in both databases. The bibliometric analysis revealed the representativeness of scientific publications, both from a global perspective (Table 2) and in their distribution over time (Figure 1). The graph showing the volume of publications per year considered all publications in both databases, excluding duplicate publications. Only the General, Specific I, and Specific II conditions are presented in Figure 1 since the Specific III condition did not presented results in both databases.

Despite the growing number of publications on CLT–concrete structures, there is still a need for further improvement in the study scenarios related to the application of CFRP connectors and parametric analyses. Moreover, there is a noticeable gap in research focused on the sensitivity analysis of parameters for CLT–concrete structures across the available databases.

Two of the four studies identified through the Specific I string applied CFRP as a reinforcing element in the tensile portion of CLT–concrete panels. Baek et al. [23] conducted bending strength tests on CLT–concrete panels and observed that the reinforcement suppressed rupture in the defect in the outermost tensile laminae of the CLT. This reinforcing effect increased the reliability of bending performance. Song et al. [24] also conducted four-point bending tests on CLT–concrete slabs reinforced with CFRP to improve their mechanical performance and reliability.

Hadigheh and Dias-da-Costa [22] conducted shear tests to investigate the performance of notched and notched connections with CFRP laminates. They determined stiffness and strength by evaluating load–slip behavior and load capacity. The results showed that adding CFRP to the connection can improve its shear strength and stiffness.

Table 2. Volume of prospected documents according to different conditions and databases.

Condition	Scopus	Web of Science
General	104	55
Specific I	4	4
Specific II	3	2
Specific III	0	0
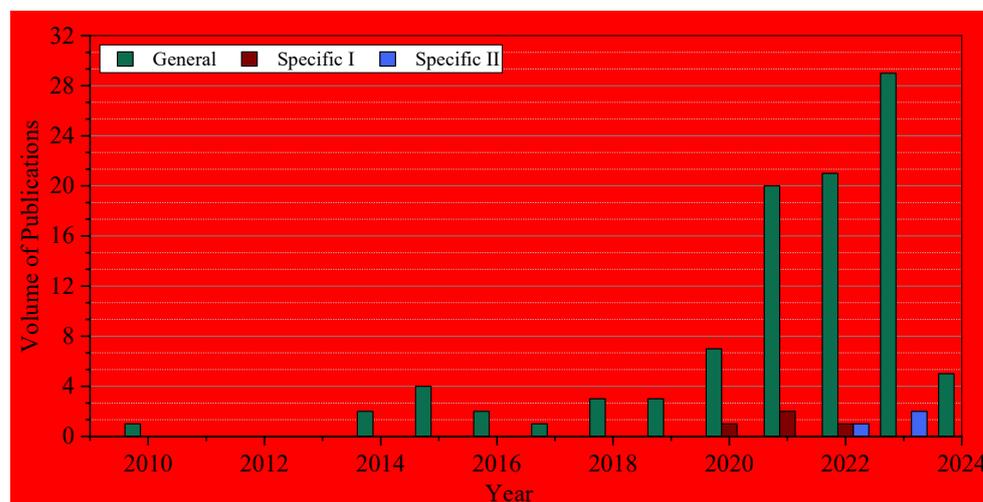
Figure 1. Annual volume of publications in the Scopus and Web of Science databases.

Only one study [6] presented the application of CFRP rebars as mechanical connectors for CLT–concrete structures. Hadigheh et al. [6] proposed the use of CFRP plates and rebars as shear connectors in CLT–concrete beams to replace conventional steel connectors. The structure's performance was assessed using four-point bending tests. The samples with CFRP rebars presented greater bending strength and stiffness in the elastic stage and ductility at failure, indicating that CFRP rebars can be adopted as an alternative to traditional steel shear connectors.

Hadigheh et al. [6] observed an increase of 16.12% in the load capacity of samples with CFRP rebars compared to samples with steel screws. The authors also highlighted an increase of 4.6% in ductility and 13.5% in bending stiffness. Furthermore, Hadigheh et al. [6] also conducted a cost evaluation to compare the feasibility of CFRP connectors. Although steel screw connections are 15.5% cheaper than CFRP rebars, CFRP composites typically show higher resistance to moisture and aggressive environments, and greater stiffness and resistance, which can compensate for their higher initial cost over the useful life of TCC systems. Therefore, these findings demonstrated the feasibility of using CFRP as shear connectors. Additionally, the observed increase in load capacity, along with improvements in bending stiffness and ductility, highlighted the need for further investigations. These investigations should consider the impact of various physical, geometric, and mechanical configurations on the structural performance of CLT–concrete composites.

Considering both databases, three documents were available in the Specific II condition [8,25,26]. Bao et al. [8] investigated the structural performance of CLT–concrete slabs through four-point bending and shear tests to evaluate the slabs' strength, stiffness, and ductility. The parameters assessed in the push-out tests were the number of CLT layers, screw embedment length, thickness of the concrete slab, connector insertion angle (45° and 90°), and screw diameter. While in the bending tests, the parameters evaluated were the number of CLT layers, slab span, screw diameter and spacing, and the height–span relationship. In addition, a parametric finite element analysis was carried out to evaluate the influence of screw spacing and arrangement on the mechanical performance of the CLT–concrete slabs.

Ouch et al. [25] conducted experimental and numerical simulation shear tests to investigate the behavior of CLT–concrete slab notched connections and performed a parametric study using a finite element model. The authors evaluated the influence of the following parameters in strength and stiffness of CLT–concrete panels: concrete strength and slab thickness, the distance between the end face of the slab and the center of the external notch, the notch dimension, and the cross-sectional area of the rebar within the notched connection.

Nguyen, Sorelli and Blanchet [26] investigated the effect of concrete shrinkage on the deflection of CLT–ultra-high-performance concrete (UHPC) slabs during the first 28 days after concreting, focusing on scenarios without shoring. Furthermore, a simplified analytical model was developed to predict slab deflection at an early age. A parametric analysis using the analytical tool was conducted to estimate the maximum span of CLT–UHPC slabs without shoring. For larger spans, the analysis also determined the optimal time for shoring removal.

Therefore, the systematic review revealed a significant shortage of studies on using CFRP connectors in CLT–concrete structures. Since the use of CFRP as a shear connector is still in its early stages, further research is crucial to gain a deeper understanding of its mechanical behavior. Furthermore, the systematic review uncovered a significant lack of parametric studies and parameter sensitivity analyses related to the structural performance of CLT–concrete systems.

Understanding how different parameters affect the behavior of the structure allows for a better assessment of the risks associated with the project. However, since no available analytical formulations can identify the relevance hierarchy between parameters in CLT–concrete structures, studies on parameter sensitivity analyses are highly relevant. Sensitivity analysis helps determine which parameters have the most significant impact on structural performance, allowing engineers and designers to focus their efforts on optimizing these parameters to improve the global performance of the structure.

The design and optimization of CLT–concrete composite structures require a detailed understanding of how various parameters influence their structural performance. Thus, this study aims to evaluate the structural performance of CLT–concrete panels using CFRP rebars as mechanical connectors through numerical simulation (physical, geometric, and contact nonlinearity) via the finite element method (FEM). A parameter sensitivity analysis was conducted based on a parametric study developed after calibrating the numerical model based on experimental results from the related literature. Furthermore, this study also proposes to determine multiple linear regression equations that can predict key performance metrics based on critical parameters. To achieve this, the considered parameters were the connector material (steel and CFRP), the number of CLT layers (3 and 5), the connector insertion angles (30° and 45°), and the connector embedment lengths (80 and 100 mm).

2. Materials and Methods

In the present research, the numerical model and mesh test were validated and evaluated using ABAQUS version 6.11 software based on the experiments carried out by Bao et al. [8].

Several studies have found that the stiffness and strength of CLT–concrete composite structures are significantly affected by the angle of the connectors [10–12,14,15] and the length of connector embedment [8,10,12]. Furthermore, increasing the cross-sectional height of CLT panels [17] and CLT in CLT–concrete systems [8] also influences the stiffness and strength of the structural system. Therefore, to assess the structural performance of CLT–concrete panels with CFRP and steel connectors, various other parameters were also altered. These included the connector's insertion angle and embedment length, as well as the number of CLT layers.

2.1. Geometric Characteristics of the Model

The constituent elements (concrete layer; CLT panel; connectors) of the CLT–concrete panels were evaluated using the widely accepted four-point static bending method. These elements were modeled separately, considering non-linear behavior for the materials. The geometric dimensions of the test specimens and the distribution of connectors are shown in Figure 2.
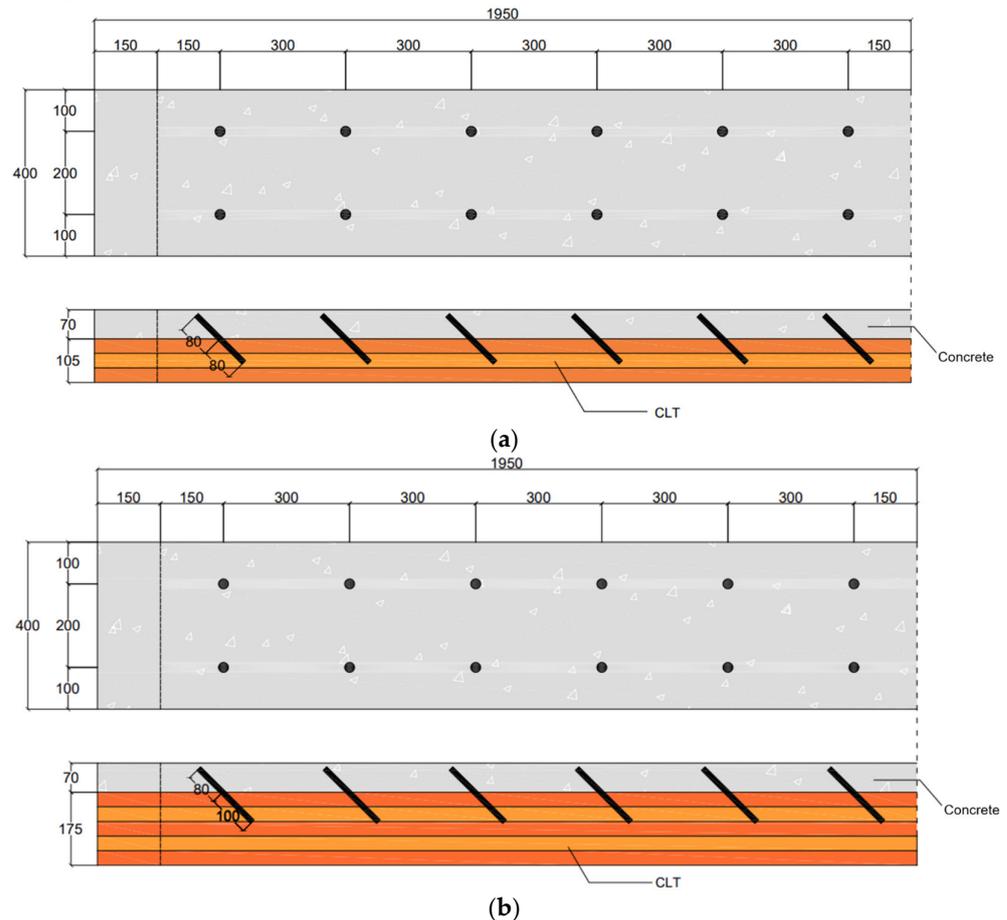
Figure 2. Geometric dimensions of the specimens with (**a**) 3 layers of CLT and connectors with an embedment length of 80 cm and (**b**) 5 layers of CLT and connectors with an embedment length of 100 cm.

2.2. Constitutive Model of Timber

Timber can be described as an orthotropic material, as it presents unique and independent mechanical properties in the longitudinal (L), radial (R), and tangential (T) directions [27]. Therefore, the CLT panel was simulated in the finite element model as an orthotropic elastoplastic material. The longitudinal elastic moduli (E) in the three axes of symmetry idealized for timber are E_L, E_R, and E_T. G_{LR}, G_{LT}, and G_{RT} are the transversal elastic moduli established for the three independent planes. As this is a computational approach, the L, R, and T axes were represented in the local coordinate system by axes 1, 2, and 3, respectively, which, in the simulations carried out, coincide with the global coordinate system x (1 or L), y (2 or R), and z (3 or T).

The orthotropic elastic properties of timber were defined according to Table 3. The E_L and Poisson's ratios were defined according to Bao et al. [8]. The relationships considered in the normative EN 338 [28], were adopted to obtain the other properties, as presented in Equations (1)–(3).

$$E_z = E_y = E_x/30 \tag{1}$$

$$G_{xy} = G_{xz} = (E_x + E_y)/32 \tag{2}$$

$$G_{yz} = (E_y + E_z)/32 \tag{3}$$

Table 3. CLT properties.

Elastic Modulus (MPa)			Poisson's Ratio			Elastic Modulus (MPa)		
E_1 [1]	E_2	E_3	ν_{12} [2]	ν_{13}	ν_{23}	G_{12}	G_{13}	G_{23}
11,000	366.667	366.667	0.48	0.48	0.48	355.208	355.208	22.917

[1] source: From [8]; [2] source: From [8].

Hill's failure criteria, developed based on the modification of the von Mises criterion (inclusion of the effects of anisotropy induced in an initially isotropic metal during the process of large plastic deformations), was used in the timber numerical simulation [29]. This criterion requires determining the six plasticity coefficients (R_{ij}) expressed in Equations (4)–(6).

$$R_{11} = \sigma_0 / \sigma_{eq} \tag{4}$$

$$R_{22} = R_{33} = \sigma_{90} / \sigma_{eq} \tag{5}$$

$$R_{12} = R_{13} = R_{23} = \sqrt{3} \cdot \sigma_v / \sigma_{eq} \tag{6}$$

In which σ_0 is the yield stress in the direction parallel to the fibers, σ_{90} is the yield stress in the direction perpendicular to the fibers, σ_v is the shear strength, and σ_{eq} is the equivalent yield stress for isotropic behavior. A bilinear constitutive model was adopted to represent the stress–strain behavior of timber [20]. The adopted value of the yield stress in the direction parallel to the fibers was 35.8 MPa [8]. The coefficients used in this study are presented in Table 4.

Table 4. R_{ij} plasticity coefficients assumed for FE simulation.

R_{11}	R_{22}	R_{33}	R_{12}	R_{13}	R_{23}
1	0.19	0.19	0.38	0.38	0.38

2.3. Constitutive Model of Concrete

The concrete damaged plasticity (CDP) model, based on the Drucker–Prager criteria, was used to consider the plastic behavior and damage of concrete [30]. It is a multiaxial constitutive model especially applicable to structural reinforced concrete. The values of the modulus of elasticity, Poisson's ratio, and average compressive strength of the concrete were adopted from Bao et al. [8], and were 30 GPa, 0.2, and 29.5 MPa, respectively. It is worth noting that the research above was used in the calibration phase of the numerical model.

In order to configure the CDP model, the following parameters were necessary: expansion angle (ψ), eccentricity (ϵ), the ratio between biaxial and uniaxial compressive yield stresses (σ_b/σ_c), shape factor (K_c), and the viscosity (μ). The values of each parameter used in this study were obtained from Laabidine, Zeineddine, and Noureddine [31], being 35°, 0.1, 1.16, 0.667, and 0.01, respectively.

2.4. Modeling of Shear Connectors

The properties of steel screws were based on a perfect elasto-plastic model. The elastic modulus and Poisson's ratio were 210 GPa and 0.3, respectively, according to Bedon and Fragiacomo [32]. The yield stress of the steel screws was 355 MPa, according to Bao et al. [8].

CFRP rebars were used as the shear connectors between timber and concrete. CFRP rebars do not have a yield point, and their behavior is linear-elastic and brittle [21]. Therefore, the yielding of CFRP rebars was not considered. This study adopted a tensile failure stress of 1784 MPa and an elastic modulus equal to 158 GPa for the CFRP rebars. As for Poisson's ratio, 0.22 was considered [31]. Both connectors were modeled as solid elements.

2.5. Numerical Model Configuration

The panels were simulated considering the boundary conditions defined by Bao et al. [8]. Due to the model's symmetrical dimensions, the numerical simulation was carried out considering a plane of symmetry in the transverse axis of the panel, aiming to improve computational performance. The model design process is illustrated in Figure 3.
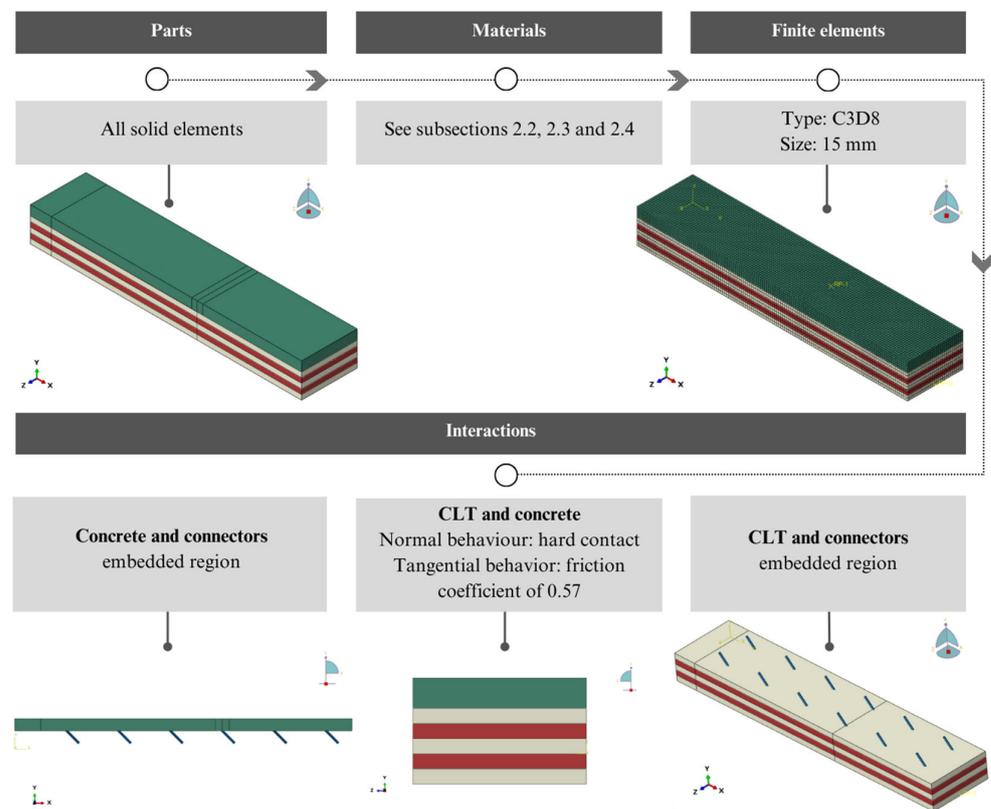
Figure 3. Steps and definition of the numerical model.

The interaction between the constituent parts of the numerical model was defined using the interaction and constraint options available in the ABAQUS software library. A perfect connection between the CLT layers was considered using the "tie" mechanical constraint option [33]. Since connectors can typically be attached to timber using epoxy adhesives or by being screwed (in the case of screws), an approximation that can be made is to assume that the interaction between the connectors and timber is ideal.

The interaction between the connectors and the CLT–concrete panel was considered using the "embedded region" option. On the CLT and concrete interface, the normal contact behavior was defined as "hard contact", while the "penalty" option was selected for the tangential behavior. The friction coefficient adopted for the interface between the CLT and the concrete was 0.57 [20].

The numerical simulation was conducted considering the application of displacements. The offset increments varied between 104 and 184, with a maximum size of 0.01.

2.6. Mesh Test

A mesh test (Figure 4) was conducted to verify the influence of the type of mesh on the model and identify the most assertive alternative for performing the numerical simulation. The parameters considered were the type and size of the mesh elements.

For CLT and concrete, models were simulated with 15 mm, 20 mm, and 25 mm mesh elements. The mesh element types were hexahedral eight-node solid elements with reduced integration (C3D8R) and without reduced integration (C3D8). Connectors were modeled with tetrahedral ten-node (C3D10) 5 mm solid elements in all mesh tests.
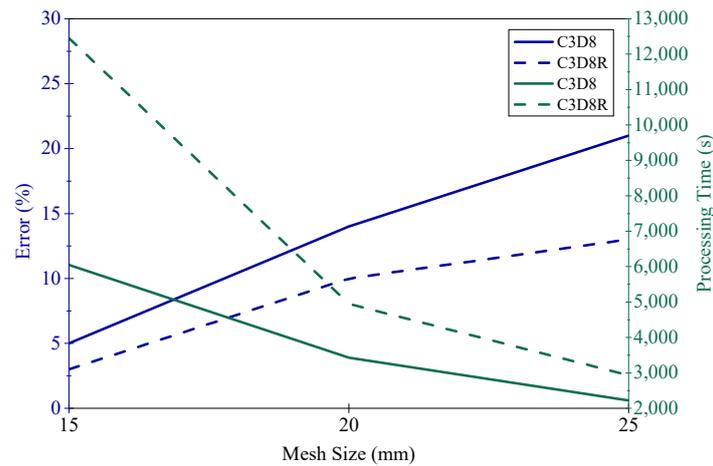
Figure 4. Mesh test graphic.

For the numerical simulations, the choice of mesh was based on two key factors: the processing time and the percentage error in comparing the maximum load obtained from the numerical simulation with that from the study used for model validation.

2.7. Parametric Study

Based on the finite element model validated for steel shear connectors, a parametric study was carried out to analyze how the mechanical performance of the CLT–concrete panel was affected by variables such as the connector material (steel screw and CFRP rebar), the connector embedment length (80 and 100 mm), the connector insertion angle (30° and 45°), and the number of CLT layers (3 and 5).

The combination of these factors resulted in 16 different numerical models (Table 5), with the CLT–concrete panels being evaluated based on the four-point static bending test structural scheme.

Table 5. Definition of parametric models.

Model	CM [1]	NC [2]	L [3] (mm)	θ [4] (°)
ST-3-80-30	Steel	3	80	30
ST-3-80-45	Steel	3	80	45
ST-3-100-30	Steel	3	100	30
ST-3-100-45	Steel	3	100	45
ST-5-80-30	Steel	5	80	30
ST-5-80-45	Steel	5	80	45
ST-5-100-30	Steel	5	100	30
ST-5-100-45	Steel	5	100	45
CFRP-3-80-30	CFRP	3	80	30
CFRP-3-80-45	CFRP	3	80	45
CFRP-3-100-30	CFRP	3	100	30
CFRP-3-100-45	CFRP	3	100	45
CFRP-5-80-30	CFRP	5	80	30
CFRP-5-80-45	CFRP	5	80	45
CFRP-5-100-30	CFRP	5	100	30
CFRP-5-100-45	CFRP	5	100	45

[1] connector material; [2] number of CLT layers; [3] connector embedment length; [4] connector insertion angles.

It is worth noting that establishing two levels for each factor was based on research by Oliveira et al. [34], who evaluated, via numerical simulation, the ultimate moment in steel–concrete beams. In this research, the authors concluded that considering only two levels of each factor investigated (32 simulations) resulted in estimates of the ultimate moment equivalent to considering 162 and 360 simulations.

2.8. Response Variables Obtained from Parametric Study Simulations

The ductility (μ) of the CLT–concrete panels was determined based on the EN 12512 standard [35], which was defined by the ratio of the displacement at the maximum load, (δ_{Fmax}) to the yield displacement (δ_y), according to Equation (7).

$$\mu = \frac{\delta_{Fmax}}{\delta_y} \tag{7}$$

The overall panels' bending stiffness can be evaluated to investigate the effectiveness of connections in distributing load between the concrete and CLT [6]. Equations (8) and (9) calculated the effective elastic bending stiffness of the panels (EI_{eff}) based on the load–displacement curves obtained from numerical simulations.

$$EI_{eff} = \frac{K_e \cdot a}{48} \cdot \left(3 \cdot L^2 - 4 \cdot a^2 \right) \tag{8}$$

$$K_e = \frac{\Delta F}{\Delta \delta} = \frac{0.4 \cdot F_{max} - 0.1 \cdot F_{max}}{0.4 \cdot \delta_{F_{max}} - 0.1 \cdot \delta_{F_{max}}} \tag{9}$$

where a is the distance from the loading point to the support, K_e is the ratio between the loading and the mid-span displacement increments, L is the panel's clear span, F_{max} is the maximum applied load, and δ_{Fmax} is the displacement correspondent.

3. Results

3.1. Validation of the Numerical Model

The numerical model was validated by reproducing the load–displacement curve from the experimental research proposed by Bao et al. [8]. Thus, Figure 5 illustrates the comparison between the results obtained in the reference study and those obtained through the model simulated during this study.
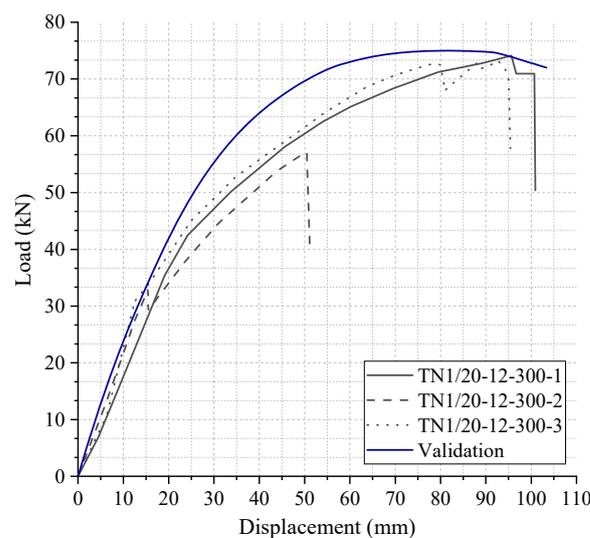
Figure 5. Comparison graphic between the results of the reference study and the simulated model.

As shown in Figure 3, the mesh with C3D8 elements and 15 mm performed best considering the analyzed parameters. Therefore, the concrete slab and the CLT were modeled using C3D8 mesh elements of 15 mm.

The final load capacity of the CLT–concrete panel predicted by the finite element model is slightly higher than the results of the reference experimental test. This can be attributed to the fact that the values adopted for certain parameters used in the model were not provided in the reference article. Because of that, the values of these properties were established following other studies in the literature. Furthermore, adopting the "tie"-type interaction attributes an idealized behavior at the interface of the CLT layers. Although commonly used, real elements do not exhibit this idealized interaction obtained by the simulation method. This may explain the difference between the idealized validation model and the experimental tests.

Despite the slight discrepancy in load capacity, the finite element model, based on the reference study [8], adequately predicted the load–displacement response of the CLT–concrete panel. This is a significant validation of the model's accuracy and its potential for future applications, as depicted in Figure 5.

3.2. Parametric Study Results

After validating the numerical model, simulations of the parametric study were carried out (Table 5). Figure 6 presents the results of the load–displacement curves, and Table 6 presents the mechanical properties obtained based on these curves.

**Table 6.** Results of load–displacement and mechanical properties.

Model	F_{max} [1] (kN)	δ_{Fmax} [2] (mm)	μ [3]	EI_{eff} [4] (kN·m^2)	f_R [5] (MPa)	M_{max} [6] (kN·m)
ST-3-80-30	80.22	60.76	1.71	2664.72	22.59	46.13
ST-3-80-45	79.19	66.07	1.91	3066.63	22.30	45.53
ST-3-100-30	81.00	60.84	1.80	2687.25	22.81	46.57
ST-3-100-45	81.39	62.14	1.65	3260.69	22.92	46.80
ST-5-80-30	152.01	97.14	1.60	3563.66	21.84	87.40
ST-5-80-45	151.27	103.26	1.74	3551.49	21.74	86.98
ST-5-100-30	152.83	97.19	1.68	3585.61	21.96	87.88
ST-5-100-45	153.76	101.53	1.60	4002.63	22.09	88.41
CFRP-3-80-30	87.73	62.06	1.64	2550.60	24.71	50.44
CFRP-3-80-45	89.42	63.32	1.69	2969.43	25.18	51.41
CFRP-3-100-30	89.57	62.20	1.69	2598.77	25.23	51.50
CFRP-3-100-45	92.26	61.46	1.53	3051.13	25.98	53.05
CFRP-5-80-30	159.96	83.07	1.30	3406.79	22.98	91.98
CFRP-5-80-45	163.31	82.18	1.29	3834.74	23.47	93.90
CFRP-5-100-30	162.55	82.16	1.24	3451.02	23.36	93.47
CFRP-5-100-45	167.78	80.28	1.27	3928.98	24.11	96.47

[1] F_{max}, maximum load; [2] δ_{Fmax}, mid-span displacement at the maximum load; [3] μ, ductility; [4] EI_{eff}, effective bending stiffness; [5] f_R, bending strength; [6] M_{max}, maximum bending moment.

Figure 6a illustrates the load–displacement curves of all simulated models, revealing four sets of similar curves. This grouping is mainly attributed to two parameters: the number of CLT layers and the material of the shear connectors. Modifying either the number of CLT layers or the connector material leads to a more pronounced alteration in the behavior of the CLT–concrete panels.

Figure 6b displays the load–displacement curves of the panels with steel connectors. The panels with five layers of CLT demonstrated a maximum load 89.5% higher than panels with three layers, 152.5 and 80 kN, respectively. The average displacement at the maximum load was 59.8% greater for the five-layer panels. For panels with CFRP connectors (Figure 6c), the maximum load was 82.1% for panels with five layers compared

to those with three layers, 163.4 and 89.7 kN, respectively. The panels with five layers showed an increase of 31.6% in the average displacement at the maximum load. The results were similar to those observed by Bao et al. [8], where increasing the number of CLT layers from three to five provided a 42.6% increase in resistance.
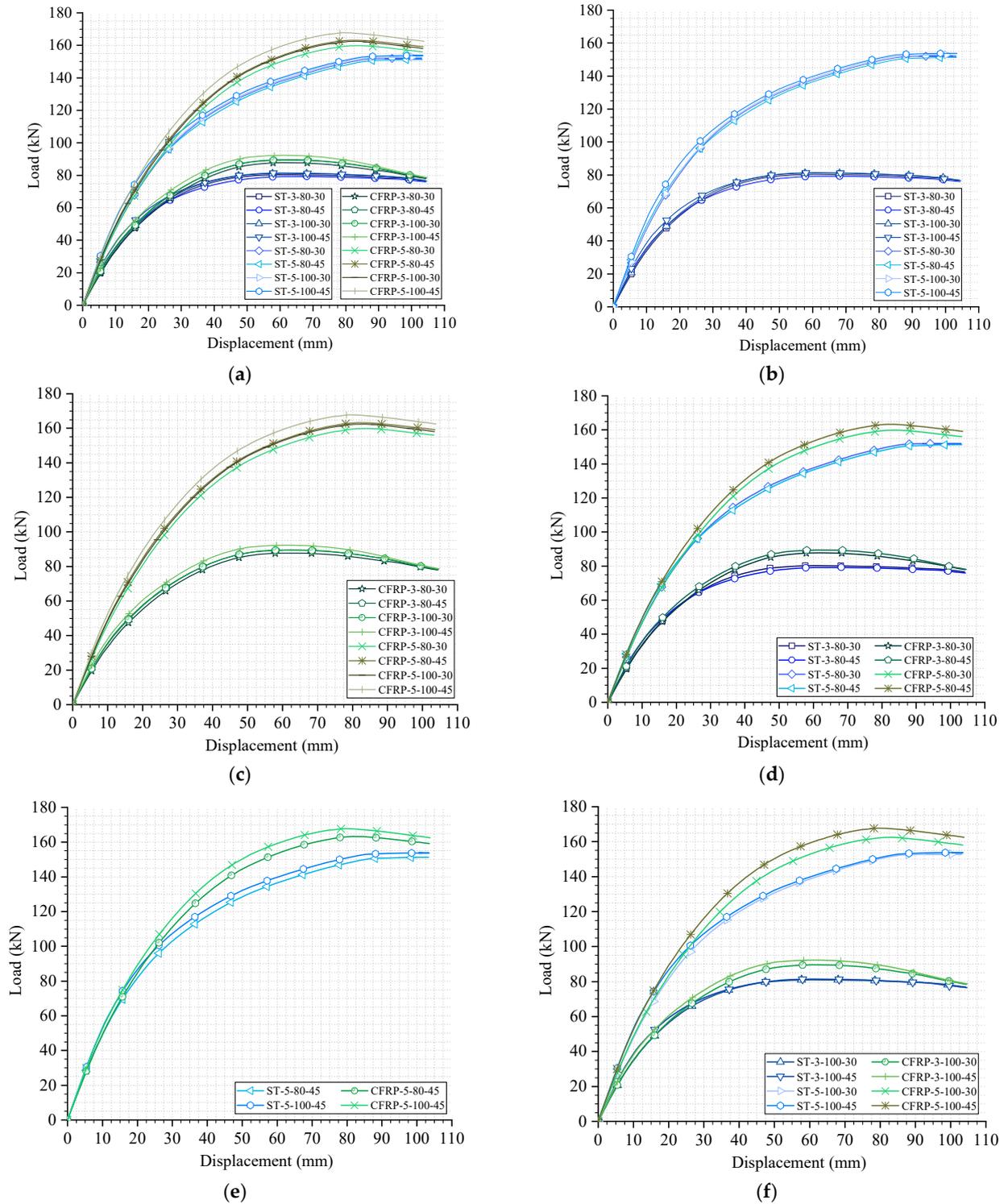
Figure 6. Load–displacement curves: (**a**) all numerical models; (**b**) numerical models with steel connectors; (**c**) numerical models with CFRP connectors; (**d**) numerical models with an embedment length of 80 mm; (**e**) numerical models with 5-layer CLT and 45° angle connectors; (**f**) numerical models with embedment length of 100 mm.

In Figure 6a,d, it is possible to observe the influence of the variation in the connector material. Figure 6d shows that the panels with CFRP connectors supported a more significant maximum load than those with steel connectors. The results are consistent with the findings of Hadigheh et al. [6]. The CFRP-3-80-30 panel supported a maximum load 9.4% greater than the ST-3-80-30, while the CFRP-5-80-30 panel supported a maximum load 5.2% greater than the ST-5-80-30. When considering three-layer panels, those with CFRP connectors presented a maximum load 11.6% higher than panels with steel connectors. For five-layer panels with CFPR connectors, these presented a maximum load 7.2% higher than panels with steel connectors. The percentages found are close to those obtained by Hadigheh et al. [6], with the exception of panels with three lamellas, which may indicate that the transfer of efforts between the concrete and the CLT starts to play a more effective role in the system when analyzing elements with a smaller cross-sectional area. A similar behavior was observed by Bao et al. [8].

In Figure 6e, the ST-5-100-45 model exhibited a maximum load 1.6% higher and a displacement 1.7% lower than the ST-5-80-45 panel. Similarly, the CFRP-5-100-45 panel presented a maximum load 2.7% higher and a displacement 2.3% lower than the CFRP-5-80-45. Generally, panels with connectors featuring a 100 mm embedment length demonstrated a slightly higher maximum load and lower displacement compared to panels with an 80 mm embedment length.

As shown in Figure 6d, panels with steel connectors and 80 mm embedment length inserted at 30° exhibited a slightly higher maximum load than panels with connectors inserted at 45°. In contrast, panels with CFRP connectors and 80 mm embedment length inserted at 45° presented a higher maximum load than panels with connectors at 30°. In Figure 6f, conversely, panels with connector embedment lengths of 100 mm and inserted at 45° provided a higher maximum load than panels with connectors inserted at 30°, regardless of the connector material.

The results presented in Table 6 show that the panels with steel connectors exhibited an average ductility 17.4% higher than the models with CFRP rebars. The median ductility value for panels with steel screws was 1.70, while it was 1.42 for panels with CFRP rebars, indicating a 19.6% difference between these values. These percentage variations were higher than those observed by Hadigheh et al. [6], indicating that the other parameters considered in this parametric study contributed to a more effective use of CFRP connectors. This is further explored in the correlation analysis of the findings presented in Section 3.3.

Considering only the variation in the number of CLT layers, the panels with three layers presented an average ductility of 1.70 and a median of 1.69. In contrast, the five-layer panels presented an average ductility of 1.46 and a median of 1.45, a percentage difference of approximately 16.0%.

Regardless of the material connector, number of CLT layers, and connector insertion angle, panels with connectors featuring an 80 mm embedment length had an average ductility of 1.63 and a median of 1.67. In comparison, panels with a 100 mm embedment length had an average ductility of 1.54 and a median of 1.60.

The connector angle had no discernible impact on the ductility values. The panels with connectors set at 30° exhibited an average ductility of 1.58 and a median of 1.66, whereas panels with connectors set at 45° showed an average ductility of 1.59 and a median of 1.62.

In Table 6, the panels with steel screws and CFRP rebars showed a similar average effective bending stiffness. The average effective bending stiffness of the panels with steel screws was 3297.8 kN·m^2, with a median of 3406.1 kN·m^2. The panels with CFRP rebars had an average effective bending stiffness of 3223.9 kN·m^2, with a median of 3229.0 kN·m^2.

When evaluating the variation in the number of CLT layers, panels with five layers exhibited an average effective bending stiffness 28.3% higher (3665.6 kN·m^2) compared to panels with three layers (2856.2 kN·m^2), with a median 26.4% higher (3574.6 kN·m^2 and 2828.3 kN·m^2, respectively).

Regardless of the connector material, number of CLT layers, and connector angle, the average effective bending stiffness of the panels with connectors having an embedment length of 100 mm was 3.7% higher than those with an embedment length of 80 mm.

Regarding the connector angle, the panels with connectors inserted at 45° showed higher average effective bending stiffness than panels with connectors inserted at 30°. The panels with connectors at 45° presented an average effective bending stiffness 12.9% higher than panels with connectors at 30°. Even so, it is noteworthy that the values found for maximum load, bending strength, and maximum bending moment showed little variation in the models studied. This can be explained by the fact that changing the insertion angle still allows for greater traction effort on the connector, different from what would be observed when adopting 90° connectors.

The panels with CFRP connectors exhibited an average bending strength value 9.4% higher than panels with steel connectors. Regarding the number of CLT layers, panels with five layers showed an average bending strength lower than the three-layer panels, with a difference of 5.3%. A longer connector embedment length resulted in an approximately 2.0% higher average bending strength for panels with an embedment of 100 mm. Concerning the connector angle, panels with connectors inserted at 30° resulted in an average bending strength lower than panels with connectors at 45°, with a difference of 1.3%.

The panels with CFRP connectors demonstrated an 8.7% increase in average maximum moment compared to panels with steel connectors. The higher number of CLT layers also resulted in a higher average maximum moment for panels with five layers, an increase of 85.6% compared to panels with three layers of CLT. The panels with an embedment length of 80 mm exhibited an average maximum moment of 69.2 MPa, while panels with a 100 mm embedment resulted in an average maximum moment of 70.5 MPa. Regarding the connector insertion angle, panels with connectors at 45° exhibited an average maximum moment of 70.3 MPa, while panels with connectors at 30° recorded a slightly lower average maximum moment of 69.4 MPa.

3.3. Statistical Analysis

An analysis of variance (ANOVA) was performed to determine whether there were significant differences between the mean values of the properties of interest for each parameter studied. Table 7 presents the results of Tukey's mean comparison test regarding the influence of the levels of the four experimental factors on the response variables of interest.

Table 7. Results of Tukey's test of mean contrast [11].

Prop.	CM [7]		NC [8]		L (mm) [9]		θ (°) [10]	
	Stell (0)	CFRP (1)	3	5	80	100	30	45
F_{max} [1] (kN)	A	A	B	A	A	A	A	A
δ_{Fmax} [2] (mm)	A	A	B	A	A	A	A	A
μ [3]	A	B	A	B	A	A	A	A
EI_{eff} [4] (kN·m²)	A	A	B	A	A	A	A	A
f_R [5] (MPa)	B	A	A	A	A	A	A	A
M_{max} [6] (kN·m)	A	A	B	A	A	A	A	A

[1] F_{max}, maximum load; [2] δ_{Fmax}, mid-span displacement at the maximum load; [3] μ, ductility; [4] EI_{eff}, effective bending stiffness; [5] f_R, bending strength; [6] M_{max}, maximum bending moment; [7] connector material; [8] number of CLT layers; [9] connector embedment length; [10] connector insertion angles; [11] of the Tukey test (5% significance), equal letters imply different treatments with means that are statistically equivalent to each other, and different otherwise, with A being greater than B.

The analysis in Table 7 reveals that the previously mentioned percentage variations in effective bending stiffness, maximum bending moment, maximum load, and displacement at the maximum load were not significant concerning the connector material type. Con-

versely, panels with steel connectors exhibited significantly greater ductility than panels with CFRP connectors. On the other hand, panels with CFRP connectors demonstrated significantly higher average bending strength compared to panels with steel connectors.

Turning to the number of CLT layers, panels with five layers exhibited a significantly higher maximum load and corresponding displacement than panels with three layers. The same was observed for the effective bending stiffness and maximum moment of the panels, where panels with five layers showed significantly higher average values than the three-layer panels. Conversely, the panels with three-layer CLT exhibited significantly higher average ductility.

Table 7 shows that the 20 mm variation in connector embedment length did not significantly differ from the mean values of the studied properties. The same was observed for the 15° variation in connector insertion angle.

Pearson coefficients were determined to assess the linear relationship between the studied parameters and the properties of interest. Table 8 presents the results of the Pearson correlation test between the properties measured in the simulations and the four independent variables (CM, NC, L, θ).

Table 8. Results of the Pearson correlation test ($-1 \leq r \leq 1$).

Parameters	F_{max} [1] (kN)	δ_{Fmax} [2] (mm)	μ [3]	EI_{eff} [4] (kN·m^2)	f_R [5] (MPa)	M_{max} [6] (kN·m)
CM [7]	0.137 [11]	−0.288	<u>−0.648</u>	−0.079	<u>0.808</u>	0.137
NC [8]	<u>0.989</u>	<u>0.908</u>	<u>−0.603</u>	<u>0.870</u>	−0.490	<u>0.989</u>
L [9]	0.031	−0.040	−0.133	0.129	0.176	0.031
θ [10]	0.021	0.059	0.006	0.424	0.111	0.021

[1] F_{max}, maximum load; [2] δ_{Fmax}, mid-span displacement at the maximum load; [3] μ, ductility; [4] EI_{eff}, effective bending stiffness; [5] f_R, bending strength; [6] M_{max}, maximum bending moment; [7] connector material; [8] number of CLT layers; [9] connector embedment length; [10] connector insertion angles; [11] Correlation coefficients (r) considered significant by analysis of variance (ANOVA, 5% significance) are underlined.

In Table 8, the connector material and the number of CLT layers showed significant linear correlations with the properties of interest.

3.4. Influence of the Connector Material on the Structural Performance of the Panels

The panels with CFRP connectors demonstrated a superior capacity to withstand maximum loads and corresponding displacements compared to CLT–concrete panels with steel connectors. The use of CFRP connectors increased maximum loads by 5.2% to 13.4% and corresponding displacements by 1.1% to 20.9%. However, Table 8 reveals no significant linear correlation between these variables.

The panels with CFRP connectors exhibited higher bending strength and maximum bending moment than panels with steel connectors, with an increase ranging from 5.2% to 13.4%. There was a significant linear correlation between the connector material and the bending strength of the panels, but this was not observed for the maximum moment.

The panels with steel connections demonstrated an effective bending stiffness of about 1.9% to 6.9% higher than those with CFRP connectors and ductility between 4.3% and 35.5% higher. The exception was the ST-5-80-45 panel, which showed lower effective bending stiffness than the CFRP-5-80-45 panel. According to Table 8, there is no significant linear correlation between the connector material and effective bending stiffness; however, there is a significant correlation between this parameter and the ductility of the CLT–concrete panels.

Similarly, through four-point bending tests, Hadigheh et al. [6] observed that CLT–concrete beams with crossed CFRP connectors exhibited higher maximum loads than beams with crossed steel connectors. However, the authors found greater ductility and effective bending stiffness for beams with CFRP connectors compared to beams with steel screws. Through shear tests, Hadigheh and Dias-da-Costa [22] also observed that CFRP connectors provided greater shear strength, stiffness, and higher ductility. Further

studies are imperative to explore the bending performance of CLT–concrete structures with CFRP connectors and their impact on the stiffness and ductility of such structures. The subsequent research could focus on developing numerical simulations and experimental tests incorporating crossed CFRP connectors with various connector spacings.

CFRP rebars used as shear connectors have demonstrated satisfactory structural performance. They offer several practical benefits over traditional steel connectors. The corrosion-resistant nature of CFRP connectors reduces the frequency of maintenance and replacements, resulting in lower long-term maintenance costs. Additionally, the lightweight properties of CFRP connectors simplify handling and installation, potentially decreasing labor costs and installation time. The high strength-to-weight ratio can enhance the overall structural performance of CLT–concrete systems by reducing the structure's weight, which is especially beneficial for seismic design or high-rise buildings.

3.5. Influence of the Number of CLT Layers on the Structural Performance of Panels

Regarding the variation in the number of CLT layers, panels with five layers withstood higher maximum loads and corresponding displacements than three-layer panels, resulting in an increase of 81.5% to 91.0% in maximum load values and 30.6% to 63.4% in corresponding displacement values. According to Table 8, these variables showed a significant linear correlation.

Increasing the number of CLT layers also resulted in higher values of effective bending stiffness and maximum bending moment. The panels with five layers showed an increase of 15.8% to 33.7% in the effective bending stiffness and an increase of 81.5% to 91.0% in the maximum bending moment. Both dependent variables (EI_{eff} and M_{max}) showed a significant linear correlation with the independent variable NC.

The panels with five layers exhibited lower bending strength and ductility than panels with three layers. The panels showed a reduction in bending strength values ranging from 2.6% to 8.0%, and a reduction in ductility values ranging from 3.1% to 36.3%. Table 8 reveals a significant linear correlation between the number of CLT layers and ductility; however, the correlation was not significant for the bending strength of the CLT–concrete panels.

Sikora, Mcpolin, and Harte [17] conducted four-point bending tests on CLT-only panels and observed a similar result. A general trend of decreasing CLT bending strength with increasing panel thickness was observed while the effective bending stiffness increased. Bao et al. [8] also observed an increase in effective bending stiffness and maximum load with the increasing number of CLT layers in CLT–concrete panels.

In this study, it was observed that three-layer panels exhibited higher ductility than five-layer panels, for both steel and CFRP connectors.

3.6. Influence of the Connector Insertion Angle on the Structural Performance of the Panels

Overall, panels with connectors at a 45° insertion angle demonstrated higher maximum load and bending strength values than panels with connectors at 30°, with a variation of only 0.5% to 3.2% higher. However, there were two exceptions: the ST-3-80-30 and ST-5-80-30 panels. Regarding the displacement at the maximum load, panels with connectors at 45° exhibited larger displacements, about 2.0% to 8.6%, compared to panels with connectors at 30°. However, there were exceptions, as the CFRP-3-100-45, CFRP-5-80-45, and CFRP-5-100-45 panels exhibited lower displacement values than the corresponding steel connection panels.

The panels with connectors inserted at 45° showed higher effective bending stiffness values, exhibiting an increase of 11.6% to 21.3% compared to panels with connectors at 30°. The only exception was the ST-5-80-30 panel, which presented slightly higher effective bending stiffness than the ST-5-80-45 panel. Additionally, the insertion of connectors at 45° increased the maximum bending moment of the panels, varying from 0.5% to 3.2% compared to panels with connectors at 30°.

In this study, the influence of the connector insertion angle on ductility values was unclear. According to Table 8, the connector insertion angle did not show a significant linear

correlation with the panels' properties under analysis. Through four-point bending tests, Mai et al. [15] observed that the bending stiffness and bending strength of the specimens were higher while the slip was lower when the screw insertion angle was 45° compared to screws at 90°. Meanwhile, in a study by Taylor, Barbosa, and Sinha [14], 45-degree screws demonstrated increased force capacity compared to 90-degree screws, with no statistically significant difference in stiffness between the two screw angles.

In experimental shear connection tests, Mirdad and Chui [12] found that screw connections with a 30° insertion angle demonstrated higher shear stiffness and strength compared to those with screws inserted at a 45° angle. Similarly, through push-out tests, Mai, Park, and Lee [10] investigated the performance of connections in CLT–concrete systems with conventional steel connectors. They observed that the use of inclined connectors (45°, 60°, and 75°) was more effective than using a vertically placed connector, with the 45° specimens exhibiting the highest stiffness. A nonlinear finite element analysis was also conducted to simulate the slip behavior under shear load. Therefore, as there are few studies that evaluate the bending performance of CLT–concrete panels with connectors inserted at a 30-degree angle, further research is necessary.

3.7. Influence of Embedment Length on the Structural Performance of Panels

The panels with connectors having an embedment length of 100 mm exhibited a slightly higher bending strength and effective bending stiffness than panels with an embedment length of 80 mm. The panels' bending strength increased by 0.5% to 3.2%, and their effective bending stiffness increased by 0.6% to 12.7%. Table 8 demonstrates no significant correlation between the embedment length and the effective bending stiffness or between the embedment length and the bending strength.

Mirdad and Chui [12] conducted shear connection tests and observed similar results, where screws with greater embedment length exhibited higher stiffness and shear strength. Bao et al. [8] also observed that increasing the embedment length of screws could significantly improve the shear performance of the connectors.

Regarding ductility, panels with connectors having an embedment length of 80 mm exhibited an increase of 1.6% to 10.5% compared to panels with an embedment length of 100 mm. The only exception was the CFRP-3-80-30 panel, which showed lower ductility than the CFRP-3-100-30 panel. Increasing the embedding length reduced the displacement at the maximum load by 1.1% to 5.9%. On the other hand, it increased by 0.5% to 3.2% in the maximum load and bending moment. According to Table 8, no significant linear correlation was observed between embedment length and the properties of interest.

3.8. Multiple Linear Regression

Equations (10)–(15) present the multiple regression models for estimating the response variables and the coefficients of determination (R^2). Figure 7 shows the Pareto graphics for each of the multiple linear regression models. The Pareto graphics enable the identification of the significance and order of significance of each factor on the estimated mechanical properties.

$$F_{max} \text{ (kN)} = -43.26 + 10.114 \cdot CM + 36.418 \cdot NC + 0.1127 \cdot L + 0.1043 \cdot \theta$$
$$R^2 = 99.90\%$$
(10)

$$\delta_{Fmax} \text{ (mm)} = 25.2 - 9.03 \cdot CM + 14.25 \cdot NC - 0.063 \cdot L + 0.124 \cdot \theta$$
$$R^2 = 91.23\%$$
(11)

$$\mu = 2.416 - 0.2550 \cdot CM - 0.1187 \cdot NC - 0.00262 \cdot L + 0.00017 \cdot \theta$$
$$R^2 = 80.15\%$$
(12)

$$EI_{eff} \text{ (kN·m}^2\text{)} = 153 - 73.9 \cdot CM + 404.7 \cdot NC + 5.99 \cdot L + 26.31 \cdot \theta$$
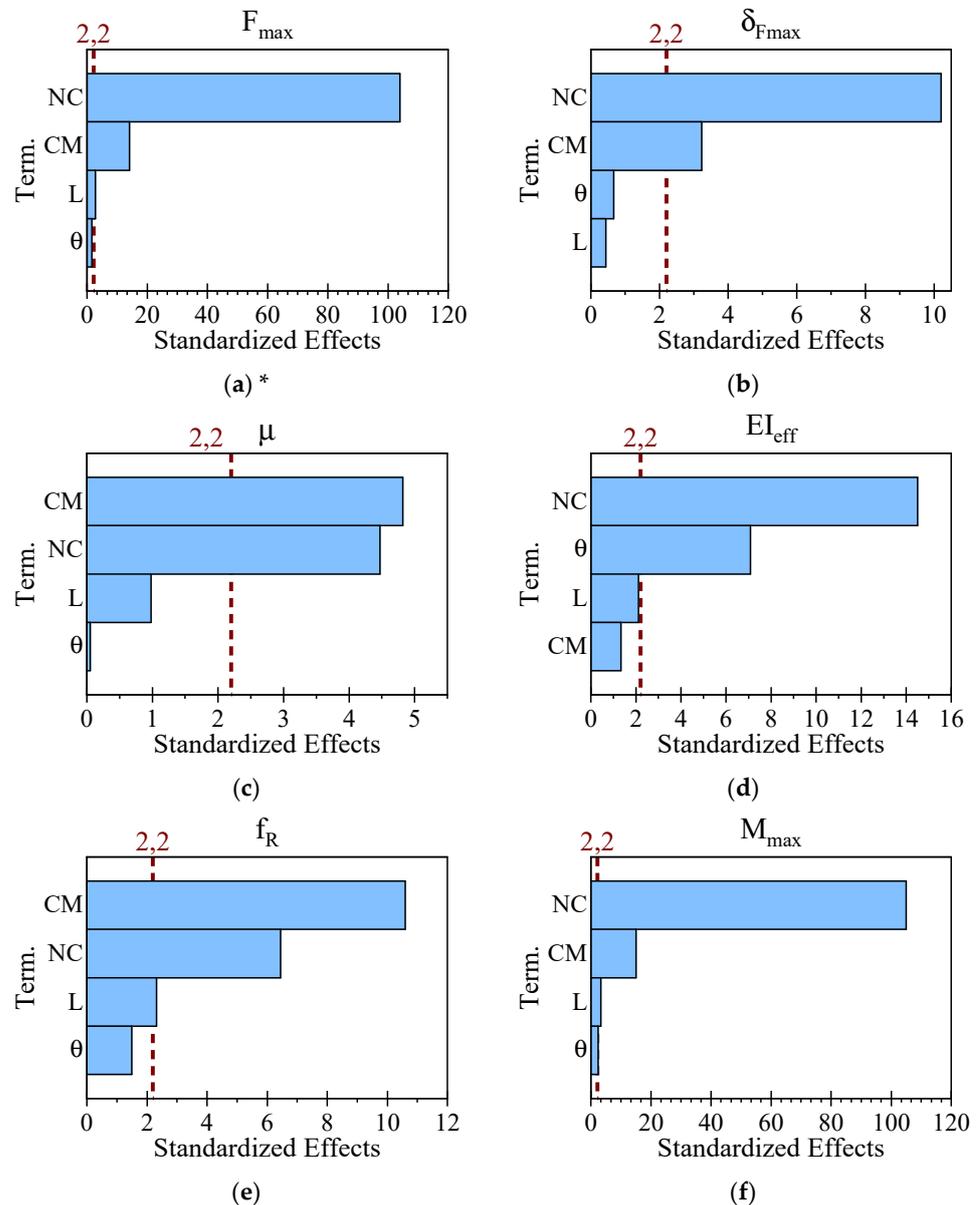$$R^2 = 96.08\%$$
(13)

$$f_R \text{ (kN)} = 22.05 + 2.096 \cdot CM - 0.6356 \cdot NC + 0.02281 \cdot L + 0.0192 \cdot \theta$$

$$R^2 = 93.64\%$$

(14)

$$M_{max} \text{ (kN·m)} = -24.88 + 5.815 \cdot CM + 20.941 \cdot NC + 0.0649 \cdot L + 0.0598 \cdot \theta$$

$$R^2 = 99.90\%$$

(15)

Figure 7. Pareto graphics of regression models: (**a**) Equation (10); (**b**) Equation (11); (**c**) Equation (12); (**d**) Equation (13); (**e**) Equation (14); (**f**) Equation (15). * Factors associated with horizontal rebars located to the right of the Pareto line are considered significant by analysis of variance (5% significance).

The high explanatory power of the regression models in this study underscores the robustness of the numerical simulations conducted using Abaqus. The high R^2 values for maximum load and bending moment reflect the precise modeling of directly measurable properties with simpler relationships. In contrast, the lower R^2 values for ductility and displacement highlight the complexity of these properties and the sensitivity to other influencing factors not initially included in this parametric study. Even so, an R^2 of 80.2%

obtained in a highly complex model is considered positive and attests to the contribution of the proposed model to estimating these properties.

According to Figure 7, the number of CLT layers, the connector material, and the embedment length are the most significant parameters for the maximum load capacity of CLT–concrete panels, with the embedment length of the connectors being the least significant parameter. Regarding the displacement at the maximum load at mid-span, the number of CLT layers and the connector material are the significant parameters. Concerning the ductility of the panels, the most relevant parameters are also the connector material and the number of CLT layers, with the connector material being the most significant.

The insertion angle of the connectors was significant only for the effective bending stiffness. The number of CLT layers was the most significant parameter for this property. For the panels' bending strength and maximum bending moment, the number of CLT layers and the connector material were the most significant parameters, and the embedment length was slightly significant for both properties.

The finding that the number of CLT layers significantly influences mechanical properties can guide the design of CLT–concrete panels for different applications. For example, designers can opt for five-layer CLT panels in structures requiring higher load-bearing capacity and stiffness, such as in multi-story buildings. The superior performance of CFRP connectors in terms of maximum load, bending strength, and maximum bending moment suggests that CFRP can be preferred in projects where these attributes are critical. In contrast, the use of steel connectors might be advantageous in scenarios where ductility and effective bending stiffness are prioritized. Longer embedment lengths and connectors inserted at 45° provide better mechanical performance in terms of load capacity and stiffness. These insights can optimize the design of connections in CLT–concrete structures, enhancing their overall reliability and safety.

4. Conclusions

Based on the results obtained in this study, the following can be concluded:

- According to the sensitivity analysis of parameters, the number of CLT layers and the connector material are the most significant parameters for the mechanical properties analyzed in this study;
- The number of CLT layers was the most significant parameter concerning the effective bending stiffness, maximum load, displacement at the maximum load, and maximum bending moment of the CLT–concrete panels;
- The panels with five-layer CLT exhibited a higher maximum load (mean value = 157.93 kN) and corresponding displacement values, as well as higher effective bending stiffness (mean value = 3665.62 kN·m^2) and maximum bending moment values (mean value = 90.81 kN·m). In contrast, panels with three-layer CLT showed better results in terms of bending strength (mean value = 23.97 MPa) and ductility (mean value = 1.70);
- The connector material was the most significant parameter for the bending strength and ductility of the CLT–concrete panels;
- The panels with CFRP connectors showed higher maximum load (mean value = 126.57 kN), bending strength (mean value = 24.38 MPa), and maximum bending moment (mean value = 72.78 kN·m) than those with steel connectors. The use of steel connectors resulted in slightly higher effective bending stiffness (mean value = 3297.84 kN·m^2) and ductility (mean value = 1.71), as well as larger displacements at the maximum load;
- The embedment length was a significant parameter for the maximum load, bending strength, and maximum bending moment of the panels;
- The panels with connectors with a longer embedment length showed better results in maximum load (mean value = 122.64 kN), bending strength (mean value = 23.56 MPa), effective bending stiffness (mean value = 3320.76 kN·m^2), and maximum bending moment (mean value = 70.52 kN·m), while panels with shorter embedment lengths showed better results in ductility (mean value = 1.62);

- The insertion angle of the connectors was a significant parameter for the effective bending stiffness of the panels;
- Connectors inserted at 45° showed better results for maximum load (mean value = 122.30 kN), bending strength (mean value = 23.47 MPa), effective bending stiffness (mean value = 3458.22 kN·m^2), and maximum bending moment (mean value = 70.32 kN·m) compared to connectors inserted at 30°;
- The multiple linear regression models for predicting the mechanical properties of interest (maximum load, displacement at the maximum load, ductility, effective bending stiffness, bending strength, and maximum bending moment) demonstrated that the parameters analyzed in this study explain 80.15% to 99.90% of the variability in the mechanical property data studied.

Numerical simulations are essential for reducing the need for extensive experimental testing. The development of predictive equations and the use of validated numerical simulations can provide a detailed understanding of the behavior of CLT–concrete structures, reduce the need for extensive experimental testing, and facilitate efficient and cost-effective design processes. This study provides valuable information for designing and constructing CLT–concrete panels. By comprehending the influence of various parameters on structural performance, engineers and designers can optimize their designs for various applications, increasing efficiency and safety. The high explanatory power of the regression models developed in this study supports their use in predictive analyses, further assisting in the practical application of these findings.

Nevertheless, the predictive equations developed in this study are suitable for use within the range of parameters considered in the parametric study. Therefore, extrapolating beyond these ranges may result in less accurate predictions and should be approached with caution.

In summary, this research highlights the importance of studies on CLT–concrete composites and the need to develop equations that satisfactorily estimate the behavior of this material. Once validated, numerical simulation is highly valuable as it provides results close to those that would be obtained in experimental laboratory tests, enabling the development of parametric studies to better understand the influence of design parameters on certain structural variables of interest. Future research should continue to refine these models and explore additional parameters to further improve the performance and applicability of CLT–concrete systems in the construction industry. This includes examining the effects of altering the spacing and configuration of connectors along the panel, varying the height/span ratio, and evaluating the use of seven-layer CLT.

Author Contributions: Conceptualization, L.F.A. and P.d.M.P.; methodology, L.F.A., P.d.M.P. and P.I.L.G.J.; software, L.F.A., P.d.M.P. and P.I.L.G.J.; validation, L.F.A., P.d.M.P. and P.I.L.G.J.; formal analysis, L.F.A., P.d.M.P. and P.I.L.G.J.; investigation, L.F.A., P.d.M.P. and P.I.L.G.J.; resources, H.F.d.S. and E.F.; data curation, L.F.A., P.d.M.P., P.I.L.G.J. and A.L.C.; writing—original draft preparation, L.F.A. and P.d.M.P.; writing—review and editing, L.F.A., P.d.M.P., P.I.L.G.J., E.F., H.F.d.S., D.H.d.A., F.A.R.L. and A.L.C.; visualization, L.F.A. and P.d.M.P.; supervision, D.H.d.A. and A.L.C.; project administration, A.L.C. All authors have read and agreed to the published version of the manuscript.

References

1. De Araujo, V.A.; Vasconcelos, J.S.; Cortez-Barbosa, J.; Morales, E.A.M.; Gava, M.; Garcia, J.N. Can Timber Houses Be Productively Faster to Build than Other Buildings? *Rev. Arvore* **2022**, *46*, e4623. [CrossRef]
2. The John W. Olver Design Building at Umass Amherst. Available online: https://www.umass.edu/bct/about-us/the-design-building-at-umass-amherst/ (accessed on 2 January 2024).
3. Brandt, K. Locally Produced Arts Centre Puts Skellefteå in the Spotlight. 2021. Available online: https://www.swedishwood.com/about_us/news/2021/9/locally-produced-arts-centre-puts-skelleftea-in-the-spotlight/ (accessed on 15 January 2024).
4. Crielaard, R.; van de Kuilen, J.-W.; Terwel, K.; Ravenshorst, G.; Steenbakkers, P. Self-Extinguishment of Cross-Laminated Timber. *Fire Saf. J.* **2019**, *105*, 244–260. [CrossRef]
5. Siddika, A.; Al Mamun, A.; Aslani, F.; Zhuge, Y.; Alyousef, R.; Hajimohammadi, A. Cross-Laminated Timber–Concrete Composite Structural Floor System: A State-of-the-Art Review. *Eng. Fail. Anal.* **2021**, *130*, 105766. [CrossRef]
6. Hadigheh, S.A.; McDougall, R.; Wiseman, C.; Reid, L. Evaluation of Composite Action in Cross Laminated Timber-Concrete Composite Beams with CFRP Reinforcing Bar and Plate Connectors Using Digital Image Correlation (DIC). *Eng. Struct.* **2021**, *232*, 111791. [CrossRef]
7. Ilgın, H.E.; Karjalainen, M. Insights from Finnish Experts on the Construction Practices and Future Prospects of Cross-Laminated Timber (CLT). *Forests* **2024**, *15*, 31. [CrossRef]
8. Bao, Y.; Lu, W.; Yue, K.; Zhou, H.; Lu, B.; Chen, Z. Structural Performance of Cross-Laminated Timber-Concrete Composite Floors with Inclined Self-Tapping Screws Bearing Unidirectional Tension-Shear Loads. *J. Build. Eng.* **2022**, *55*, 104653. [CrossRef]
9. Dias, A.; Skinner, J.; Crews, K.; Tannert, T. Timber-Concrete-Composites Increasing the Use of Timber in Construction. *Eur. J. Wood Wood Prod.* **2016**, *74*, 443–451. [CrossRef]
10. Mai, K.Q.; Park, A.; Lee, K. Experimental and Numerical Performance of Shear Connections in CLT–Concrete Composite Floor. *Mater. Struct.* **2018**, *51*, 84. [CrossRef]
11. Mirdad, M.A.H.; Chui, Y.H.; Tomlinson, D. Capacity and Failure-Mode Prediction of Mass Timber Panel-Concrete Composite Floor System with Mechanical Connectors. *J. Struct. Eng.* **2021**, *147*, 04020338. [CrossRef]
12. Mirdad, M.A.H.; Chui, Y.H. Load-Slip Performance of Mass Timber Panel-Concrete (MTPC) Composite Connection with Self-Tapping Screws and Insulation Layer. *Constr. Build. Mater.* **2019**, *213*, 696–708. [CrossRef]
13. Marchi, L.; Scotta, R.; Pozza, L. Experimental and Theoretical Evaluation of TCC Connections with Inclined Self-Tapping Screws. *Mater. Struct.* **2017**, *50*, 180. [CrossRef]
14. Taylor, B.; Barbosa, A.R.; Sinha, A. In-Plane Shear Cyclic Performance of Spline Cross-Laminated Timber-Concrete Composite Diaphragms. *J. Struct. Eng.* **2021**, *147*, 04021148. [CrossRef]
15. Quang Mai, K.; Park, A.; Nguyen, K.T.; Lee, K. Full-Scale Static and Dynamic Experiments of Hybrid CLT–Concrete Composite Floor. *Constr. Build. Mater.* **2018**, *170*, 55–65. [CrossRef]
16. Shahnewaz, M.; Jackson, R.; Tannert, T. CLT Concrete Composite Floors with Steel Kerf Plate Connectors. *Constr. Build. Mater.* **2022**, *319*, 126092. [CrossRef]
17. Sikora, K.S.; McPolin, D.O.; Harte, A.M. Effects of the Thickness of Cross-Laminated Timber (CLT) Panels Made from Irish Sitka Spruce on Mechanical Performance in Bending and Shear. *Constr. Build. Mater.* **2016**, *116*, 141–150. [CrossRef]
18. Morrell, I.; Higgins, C.; Sinha, A.; Barbosa, A.R. Experimental Assessment of Alternative Shear Connections in Cross-Laminated Timber-Concrete Floor Systems. *J. Struct. Eng.* **2023**, *149*, 04023046. [CrossRef]
19. Shahnewaz, M.; Jackson, R.; Tannert, T. The Arbour: An Innovative Composite Floor System. In *Proceedings of the Structures Congress 2022*; ASCE: Reston, VA, USA, 2022; pp. 251–259.
20. Jiang, Y.; Crocetti, R. CLT-Concrete Composite Floors with Notched Shear Connectors. *Constr. Build. Mater.* **2019**, *195*, 127–139. [CrossRef]
21. Yun, H.-D.; Kim, S.H.; Choi, W. Determination of Mechanical Properties of Sand-Coated Carbon Fiber Reinforced Polymer (CFRP) Rebar. *Polymers* **2023**, *15*, 2186. [CrossRef] [PubMed]
22. Hadigheh, S.A.; Dias-da-Costa, D. Shear Strength of Cross Laminated Timber-Concrete Connections Reinforced with Carbon Fibre Polymer Composites. In *Proceedings of the 25th Australasian Conference on Mechanics of Structures and Materials*; Springer: Berlin/Heidelberg, Germany, 2020.
23. Baek, S.Y.; Song, Y.J.; Yu, S.H.; Kim, D.H.; Hong, S. Il Bending Performance of Cross-Laminated Timber-Concrete Composite Slabs According to the Composite Method. *BioResources* **2021**, *16*, 8227–8238. [CrossRef]
24. Song, Y.J.; Baek, S.Y.; Yu, S.H.; Kim, D.H.; Hong, S. Il Evaluation of the Bending Performance of Glued CLT-Concrete Composite Floors Based on the CFRP Reinforcement Ratio. *BioResources* **2022**, *17*, 2243–2258. [CrossRef]
25. Ouch, V.; Heng, P.; Somja, H.; Soquet, T. An Experimental and Numerical Investigation on a Dovetail Notched Connection for Cross-Laminated-Timber-Concrete Composite Slabs. In Proceedings of the World Conference on Timber Engineering (WCTE 2023), Oslo, Norway, 19–22 June 2023; Volume 6, pp. 3333–3341. [CrossRef]
26. Nguyen, T.T.; Sorelli, L.; Blanchet, P. Composite Slab Floors Made of Cross Laminated Timber and Ultra High-Performance Concrete: Early-Age Deflection, Stripping Time, and Its Implication on the Structural Performances. *Eng. Struct.* **2023**, *295*, 116810. [CrossRef]
27. Vilela, R.; Mascia, N.T. Avaliação de Propriedades Mecânicas Da Madeira de Pinustaeda Provenientes de Placas de Cross Laminated Timber. *Ambient. Construído* **2021**, *21*, 89–110. [CrossRef]

28. *EN 338*; Structural Timber—Strength Classes. European Committee for Standardization (CEN): Brussels, Belgium, 2016.
29. Christoforo, A.L.; Gomes, A.F.F.; Arroyo, F.N.; Mascarenhas, F.J.R.; dos Santos, H.F.; Topolniak, L.; Akasaki, J.L. Reinforcement of Timber Beams with Steel Bars: Parametric Analysis Using the Finite Element Method. *Buildings* **2022**, *12*, 1036. [CrossRef]
30. Silva, L.M.E.; Christoforo, A.L.; Carvalho, R.C. Calibration of Concrete Damaged Plasticity Model Parameters for Shear Walls. *Rev. Mater.* **2021**, *26*, 19. [CrossRef]
31. Laabidine, H.Z.; Zeineddine, B.; Noureddine, F. The Influence of Notch Connection Location on the Short-Term Behaviour of Timber-Concrete Composite Beams, Modelling of TCC Beams and Research for Optimal Locations, a Numerical Study. *Frat. Ed Integrita Strutt. Struct. Integr.* **2023**, *17*, 186–203. [CrossRef]
32. Bedon, C.; Fragiacomo, M. Numerical Analysis of Timber-to-Timber Joints and Composite Beams with Inclined Self-Tapping Screws. *Compos. Struct.* **2019**, *207*, 13–28. [CrossRef]
33. Kawecki, B. Guidelines for FEM Modelling of Wood-CFRP Beams Using ABAQUS. *Arch. Civ. Eng.* **2021**, *67*, 175–191. [CrossRef]
34. de Oliveira, V.M.; Prates, L.M.S.; Christoforo, A.L.; Martins, C.H.; Rossi, A.; Ferreira, F.P.V. Regression Models for Ultimate Hogging Moment Prediction of Composite Cellular Beams. *Aust. J. Struct. Eng.* **2023**, *25*, 266–277. [CrossRef]
35. *EN 12512*; Timber Structures—Test Methods—Cyclic Testing of Joints Made with Mechanical Fasteners. European Committee for Standardization (CEN): Brussels, Belgium, 2001.